HHS Public Access

Author manuscript

JACC Clin Electrophysiol. Author manuscript; available in PMC 2022 March 01.

Published in final edited form as:

JACC Clin Electrophysiol. 2021 March ; 7(3): 395–407. doi:10.1016/j.jacep.2020.09.009.

Prospective Multicenter Assessment of a New Intraprocedural Automated System for Localizing Idiopathic Ventricular Arrhythmia Origins

Shijie Zhou, PhD[1,6], **Amir AbdelWahab, MD**[2], **John L Sapp, MD**[2,4], **Eric Sung, BA**[1,6], **Konstantinos N. Aronis, MD**[3,6], **James W. Warren, BSc**[4], **Paul J. MacInnis, BSc**[4], **Rushil Shah, MBBS MHS**[3], **B Milan Horáček, PhD**[5], **Ronald Berger, MD PhD**[3,6], **Harikrishna Tandri, MD**[3,6], **Natalia A. Trayanova, PhD**[1,6,†], **Jonathan Chrispin, MD**[3,6,†]

[1]Department of Biomedical Engineering, Johns Hopkins University, Baltimore, MD, USA

[2]Department of Medicine, Queen Elizabeth II Health Sciences Centre, Halifax, NS, Canada

[3]Section of Cardiac Electrophysiology, Division of Cardiology, Department of Medicine, Johns Hopkins Hospital; Baltimore, MD, USA

[4]Department of Physiology and Biophysics, Dalhousie University, Halifax, NS, Canada,

[5]School of Biomedical Engineering, Dalhousie University, Halifax, NS, Canada,

[6]Alliance for Cardiovascular Diagnostic and Treatment Innovation, Johns Hopkins University, Baltimore, MD, USA

Abstract

Background: We previously developed an intraprocedural automated site of origin localization system to identify the origin of early left ventricular (LV) activation using 12-lead ECGs. However, it has limitations, as it could not identify the site of origin in the right ventricle (RV), and relied on acquiring a complete electroanatomic map (EAM).

Objective: The objective of this study was to present a new system, the Automatic Arrhythmia Origin Localization (AAOL) system, which utilized incomplete EAM for localization of idiopathic

Corresponding Author: Shijie Zhou PhD, School of Biomedical Engineering, Alliance for Cardiovascular Diagnostic and Treatment Innovation, Johns Hopkins University, Hackerman Hall, Suite 218, 3400 North Charles Street, Baltimore MD, US, 21218, fax 410.516,5294, shijie.zhou@jhu.edu.

[†]Co-primary investigators and senior co-authors

Conflicts of Interest:

1. Dr. John L. Sapp: a co-holder of a patent for automated VT localization; no licensing, royalties or income currently or anticipated. Research funding from Biosense-Webster and Abbott (for clinical trial of catheter ablation of VT); modest speaker honoraria Medtronic, Biosense Webster, Abbott.
2. Dr. B. Milan Horáček: a co-holder of a patent for automated VT localization; no licensing, royalties or income currently or anticipated.
3. Dr. Amir Abdel Wahab: speaker honoraria Abbott, Medtronic.

ventricular arrhythmia (IVA) origin on the patient-specific geometry of LV, RV and neighboring vessels. The accuracy of the system in localizing IVA source sites on cardiac structures where pace-mapping is challenging was assessed.

Methods: Twenty patients undergoing IVA catheter ablation had a 12-lead ECG recorded during clinical arrhythmia and during pacing at various locations identified on EAM geometries. The new system combined 3-lead (III, V2, V6) 120-ms QRS integrals and patient-specific EAM geometry with pace mapping to predict the site of earliest ventricular activation. The predicted site was projected onto EAM geometry.

Results: Twenty-three IVA origin sites were clinically identified by activation mapping and/or pace mapping (8 RV; 15 LV, including 8 from the posteromedial papillary muscle; 2 from the aortic root; and 1 from the distal coronary sinus). The new system achieved a mean localization accuracy of 3.6 mm for the 23 mapped IVAs.

Conclusions: The new intraprocedural AAOL system achieved accurate localization of IVA origin in ventricles and neighbouring vessels, which could facilitate ablation procedures for patients with IVAs. Key Words: Idiopathic ventricular arrhythmias (IVA); Premature ventricular complexes (PVCs); idiopathic ventricular tachycardia (IVT); Pace mapping; Activation mapping; Radiofrequency (RF) Ablation; ECG.

Condensed Abstract

Prior site of origin systems to identify idiopathic ventricular arrhythmias (IVA) are limited by the need to create complete electroanatomic maps (EAM), inability to localize intracardiac structures/vessels and require pre-procedural cardiac imaging. Our Automatic Arrhythmia Origin Localization (AAOL) system addresses these issues. The AAOL system combines 3-lead, 120-ms QRS integrals with pace mapping to predict the site of earliest ventricular activation and project that site onto patient-specific EAM geometry. In a prospective, multicenter study of patients undergoing IVA catheter ablation, twenty-three IVA origin sites were localized by the AAOL system with a mean localization accuracy of 3.6 mm, better than any prior published system.

Introduction

Idiopathic ventricular arrhythmias (IVAs), including idiopathic ventricular tachycardias (IVTs) and premature ventricular complexes (PVCs), occur frequently in patients without apparent clinical structural heart disease (1). IVAs have been thought to be caused by triggered activity (2) and to originate in a variety of areas within the ventricles and the neighboring vessels (3). Catheter ablation is an effective treatment (4). Three-dimensional (3D) electroanatomic mapping (EAM) to accurately identify critical sites of origin is very helpful for the success of IVA ablation (5). A number of 12-lead electrocardiogram (ECG) algorithms (6–9) and non-invasive ECG imaging (ECGI) approaches (10–11) have been used to pre-procedurally predict IVA source sites. However, using 12-lead ECG algorithms to interpret the IVA origin sites or chamber of interest may provide insufficient spatial resolution and accuracy, resulting in need for frequent ectopy to combine activation mapping (12). The localization accuracy of ECGI is moderate and still is to be incorporated into routine clinical practice (13); quantitative clinical assessment of ECGI for localizing the site of origin of PVCs/IVTs has been challenging (11).

We have previously developed an intraprocedural automated site-of-origin localization (SOLO) system (14) that consists of three consecutive independent steps, progressively approaching the identification of a VT exit site: 1) site-of-origin localization to a left ventricular (LV) segment, 2) population-based site-of-origin localization within a LV segment, and 3) patient-specific site-of-origin localization. The SOLO system was prospectively assessed in patients with scar-related VT, achieving a promising localization accuracy (mean error 7.2 ± 4.1 mm) (15). The SOLO system utilizes a generic LV model, and thus can not be used to identify the site of origin of early right ventricular (RV) activation, and relies on acquiring a complete electroanatomic mapping (EAM) geometry. Furthermore, the site-of-origin localization is based on the calculation of a vector from the LV center to the predicted site, projecting the predicted site onto EAM geometry. If this vector crosses over undulations in the LV endocardial surface, it is possible to create spurious estimates of site of origin. To overcome these limitations, we omitted the first two steps of the SOLO system, which were based on population-derived statistical analysis, and further developed and augmented the personalized third step of the SOLO system to produce a new version, automatic arrhythmia origin localization (AAOL) system, capable of finding the sites of earliest activation in both ventricles. The new system combines information from 3-lead ECG (leads III, V2, V6) recordings and intracardiac patient-specific EAM geometry (partial or full geometry), which is further incorporated into pace-mapping to accurately identify the site of earliest ventricular activation projected onto EAM geometry by using the EAM site in the triangular geometrical mesh nearest the tip-of-the-catheter predicted ablation site.

This study has three objectives: 1) to demonstrate the feasibility of the new system for localizing IVA origin sites on intracardiac EAMs of both ventricular chambers and neighboring vessels, 2) to quantitively estimate performance of the new system in identifying IVA origin sites, and 3) to assess the localization accuracy of the AAOL system in cardiac structures where the pace-mapping method can be challenging(16), such as the right ventricle (RV), aortic root and papillary muscles.

Methods

Study population

Patients undergoing catheter ablation of IVAs were recruited at two centers (Johns Hopkins Hospital and Queen Elizabeth II Health Sciences Centre) for this prospective study. The study protocol was reviewed and approved by the institutional review board (IRB) of the participating institutions. All patients gave written informed consent to participate in the study.

Data acquisition and processing

Eight independent leads (I, II, V1—V6) of the 12-lead ECG were acquired via multichannel recording system (Prucka Cardiolab, GE Healthcare, Waukesha, WI) during the electrophysiology (EP) study, filtered (0.05 to 100 Hz), and sampled at 1000 Hz with 16-bit resolution; the other 4 leads (Lead III, aVF, aVL, aVR) were simultaneously computed. The output of the amplifier and system which routinely processes the signal was cloned to an

ancillary secured computer where additional processing and analysis can be performed by the AAOL system without affecting the clinical signal. Within each 7 seconds recording during IVAs or pacing performed in sinus rhythm, an IVA or paced beat was manually selected for analysis. The AAOL system does not need a pre-acquired geometry. The QRS integrals ($\int$QRS) calculated over the initial 120 ms of the QRS complex of the 3-lead ECG (III, V2, V6) were extracted by the AAOL system and used for offline analysis. The QRS onset was automatically identified (17). Manual adjustment of the 120-ms window was performed if correction of QRS onset was necessary. In addition, Cartesian coordinates of known pacing sites and corresponding mapped IVA's intracardiac EAM geometry were exported for offline analysis.

Automatic Arrhythmia origin localization (AAOL) system workflow

During a procedure, the IVAs' standard ECGs were recorded in real time. From the acquired ECG of the IVA, a choice was made which ventricular chamber to create an 3D EAM geometry or a 3D EAM integrated with intracardiac echocardiography (CartoSound, Biosense Webster, Diamond Bar, CA). To localize the origin of the IVA, pacing was delivered at locations in the chosen chamber. From the acquired ECG of the IVA, the AAOL system calculates the 120-ms QRS integrals of a set of 3 leads (III, V2, and V6). From the ECGs of the paced activations, the 120-ms QRS integrals for the same 3 leads (III, V2, and V6) are also calculated. The QRS integrals of the paced activations are entered into multiple regression models linking them to each of the pacing sites' known coordinates X, Y, Z. Regression coefficients are determined from these models. The AAOL system uses the regression coefficients determined in a multiple regression model to predict the target coordinates ($\hat{X}$, $\hat{Y}$, $\hat{Z}$) of the IVA from the 3-lead 120-ms QRS integrals of the IVA. The predicted IVA origin site coordinates ($\hat{X}$, $\hat{Y}$, $\hat{Z}$) are projected onto the acquired partial EAM geometry using a nearest neighbor algorithm, so that the site can be targeted for ablation.

In this study, for each IVA, we tested the performance of the AAOL system for two sets of pacing sites. For the first set of pacing sites (pacing sites Distribution #1), we used all recorded pacing sites of an IVA being mapped (pacing sites at the discretion of the attending electrophysiologist), as it is done chronologically during the clinical procedure. In the second set of pacing sites (Distribution #2), we used 10 pacing sites from Distribution #1 that were closest to IVA origin. We used these two different distributions to assess the performance of the AAOL system – should Distribution #2 result in a better prediction, then the AAOL system would require knowledge of the approximate site of origin. For patients with multiple IVAs, the AAOL system reused collected pacing sites, adding a few new pacing sites collected near an anticipated IVA origin.

The AAOL system workflow in this study is presented in Fig.1. A complete description of all the steps in the AAOL algorithm and justification of all choices made in it are presented in the Online Supplementary Materials. Currently, given that the system is not integrated with a commercial mapping system, it takes a couple of minutes to transfer the 3D coordinates of the pacing sites and the EAM geometries to the ancillary secured computer with the AAOL system.

Clinical Electrophysiology (EP) Mapping and Catheter ablation

The IVA ablation procedure was performed using standard techniques (3). Access to the LV was achieved via a retrograde aortic or trans-septal approach, and to the RV via a transvenous approach. For each procedure, Carto 3 (Biosense Webster, Diamond Bar, CA) or EnSite ™ Precision (Abbott, St. Paul, MN) system was used for EAM; an EAM was created using an open-irrigated catheter (ThermoCool SmartTouch., Biosense Webster, Diamond Bar, CA; FlexAbility SE, Abbott, Abbott Park, IL) or a high-density (HD) multi-electrode catheter (PentaRay NAV Catheter, Biosense Webster; Grid Catheter, Abbott, Abbott Park, IL). The use of an image integration module (CartoSound, Biosense Webster, Diamond Bar, CA) was left to the discretion of the attending electrophysiologist. Activation mapping and pace mapping of the LV and/or RV were performed to localize the site of IVA origin sites. Pacing-site distribution was at the discretion of the operating electrophysiologist. Pacing was performed with stable catheter position at multiple sites at minimum pacing output (range: 2 milliamps (mA) to 10 mA) that ensured consistent focal myocardial capture, at which point the Carto 3 /EnSite ™ Precision mapping system was used to tag it and acquire the *x, y, z* coordinates. Radiofrequency (RF) ablation was performed using an open-irrigated catheter (ThermoCool SmartTouch., Biosense Webster, Diamond Bar, CA; FlexAbility SE, Abbott, Abbott Park, IL) when targeting the earliest activation site, pre-systolic potentials and 12/12 pace matches. Procedural success was defined as complete elimination of the clinical IVA. Partial success was defined as ≥ 50% reduction in PVC burden.

Data analysis

All IVA ablation procedures were performed by clinicians, blinded to the prediction results of the AAOL system. The IVA origin site was clinically identified by activation mapping and/or pace-mapping. Origin sites on the EAM were defined in stepwise priority as: 1) sites of successful IVA suppression with ablation, and/or 2) sites of earliest activation, and/or 3) pace-mapping sites that had the highest correlation score when activation mapping was not performed due to a low PVC burden (18). Localization of a mapped IVA was performed on an ancillary secured computer with the AAOL system. Estimated localization accuracy was quantified for the IVA origin site in millimeters, by comparing the estimated against the clinically-defined locations.

Statistical Analysis

The mean and standard deviation (SD) were used to report statistical analysis results. Two pacing-site distributions were compared by using paired *t*-test. A comparison of the localization error between RV and LV IVAs was conducted using two-sample *t*-test. A double-sided $P < 0.05$ was considered statistically significant. Statistical analysis was performed with the Minitab 18 Statistical Software (Minitab Inc, State College, PA).

Results

Patient Characteristics

A total of 22 sequential consenting patients were recruited from two centers (Johns Hopkins Hospital n=13; and Queen Elizabeth II Health Sciences Centre n=9) for this prospective

study. Two patients were excluded from final analysis due to absence of PVCs at the time of the procedure. Twenty patients (70.0% male, 59.5 ± 19.6 years) were studied and the corresponding patients' clinical characteristics are presented in Table 1. For the 20 patients, twenty-three IVA (21 PVC and 2 VTs) were mapped to both ventricular chambers and neighboring vessels, as shown in Table 2, and recorded by the AAOL system in real time. In summary, 8 IVA localized to the RV, 14 were from the LV (including 8 from the posteromedial papillary muscle, and 2 from the aortic root) and 1 was from the distal coronary sinus; IVA origin sites were clinically identified primarily with activation mapping in 19 IVA (82.61%), pace-mapping in 3 IVA (13.04%) and successful suppression with ablation in 1 IVA (4.35%) (Table 2).

Procedural Characteristics

Seventeen patients underwent an electrophysiology study with the Carto 3 (Biosense Webster, Diamond Bar, CA) mapping system, and 3 patients with the EnSite ™ Precision (Abbott, St. Paul, MN) system. Acute procedural success was achieved in 19/21 PVCs. Partial acute PVC ablation success was achieved in 2/21 PVCs. One IVT was primarily pace-mapped to the RV moderator band, however ablation was not performed because this was not the patient's clinical VT and due to the difficulty in inducing the VT; the other was successfully ablated at the region of the aorto-mitral continuity (AMC).

Localization Accuracy

Patients had 1.2 ± 0.0 IVAs; and 15.2 ± 9.1 pacing sites. The spatial resolution (i.e., the average edge length) of all 20 patient-specific anatomic geometries was 1.8 ± 0.5 mm. The 23 IVA morphologies were successfully localized onto the patient-specific EAM geometry using the AAOL system; localization errors of the 23 IVA source sites are summarized in Figure 2. Mean localization accuracy was 3.6 ± 3.0 mm when using all recorded pacing sites of the mapped IVA (Distribution #1). When including up to 10 nearest pacing sites of a clinically-identified IVA (Distribution #2), the mean accuracy was 3.6 ± 2.6 mm (Table 3). There was no statistical difference in localization error between Distribution #1 and Distribution #2 ($P > 0.05$). There was no difference in mean localization error in RV compared to LV using Distribution #1 (4.3 *vs.* 3.3 mm, $P > 0.05$, respectively) or Distribution #2 (3.9 *vs.* 3.4 mm, respectively).

In 14 cases, the PaSo™ module (Carto 3 system, Biosense webster, Diamond Bar, CA) are the AutoMap module (EnSite ™ Precision, Abbott, St. Paul, MN) were utilized to estimate the correlation coefficients between the IVA morphology and pacing-site ECG morphologies (Table 3). The average distance from the site with the highest correlation score to the AAOL-predicted site (Distribution #1) was 10.0 ± 6.3 mm.

Clinical emulation to localize the IVA origin sites

Below we describe four exemplar patients to illustrate the ability of the AAOL system to localize IVA origin sites from different anatomical locations.

Patient #6 Papillary Muscle Origin: The clinical PVC had a right-bundle-branch-block-type (RBBB) morphology, inferior axis, and was biphasic in lead I (Fig. 3A). Endocardial

EAM of LV was performed using the EnSite mapping system. Pace mapping and activation mapping was performed, with the earliest activation site found on the posteromedial papillary muscle and indicated by a yellow star on the EAM map (Fig. 3B). RF ablation lesions were applied over this area, with elimination of the PVC burden. Figure 3C shows that the AAOL system predicted accurately the site of the PVC origin on the posterolateral papillary muscle, achieving a localization accuracy of 5.0 mm when using 8 pacing sites.

Patient #10 Distal Coronary Sinus: The clinical PVC of the patient had a RBBB morphology with an inferior axis and positive concordance in all precordial leads (Fig. 4A). Activation mapping was first performed in the CS with earliest activation in the distal CS. RF ablation lesions were applied over this region with transient suppression of the PVCs. RF ablation lesions at this site were limited due to high impedance. Mapping was then performed of the LV endocardium, directly opposite the earliest site in the CS. RF ablation up to 45W was delivered at the site of earliest activation, resulting in PVC increased automaticity followed by PVC suppression. The PVC origin site was identified in the distal CS, indicated by the yellow star and the green dot on the EA map (Fig. 4B). We used all recorded 9 pacing sites within the CS EAM geometry to predict the site of PVC origin onto the distal CS, having a localization error of 1.5 mm, as shown in Fig. 4C.

Patient #12 Right Ventricular Outflow Tract: The clinical PVC had a LBBB morphology with a rightward axis, and a transition in the precordial lead at V6 (Fig. 5A). An EAM of the RVOT was created using the Carto 3 mapping system. Activation and pace mapping of the PVC was performed. Activation mapping of the PVC revealed a local pre-QRS activation (−30 ms) with QS pattern on the local unipolar electrode in the septal RVOT indicated by the yellow star and the red cross (Fig. 5B); and pace-mapping at that location was 97% PaSo correlation score.. Despite the early activation, there was a large “blush” on the EAM and thus further activation mapping was performed in the LVOT opposite the earliest site on the RVOT. The activation time was later in the LVOT. RF ablation lesions were performed at the earliest activation site in the septal RVOT and the PVC burden was eliminated. Using each of the two pacing-site distributions, the PVC was localized onto the septal RVOT region, as marked by the blue patch (Fig. 5C), respectively. The AAOL system achieved a localization accuracy of 2.5 mm using Distribution #2, in comparison to the red star site identified clinically.

Representative Patient #17 Right Coronary Cusp: The clinical PVC had a LBBB morphology, inferior axis and positive concordance in all precordial leads (Fig. 6A). The clinical PVC origin site was identified at the right sinus of Valsalva, where early activation was found 39 ms ahead of the PVC QRS onset indicated by a yellow dot on the EAM map (Fig. 6B). Ablation in the right sinus of Valsalva resulted in complete suppression of the clinical PVC. Using the AAOL system with two pacing-site distributions, the estimated clinical PVC origin site was accurately localized onto the right sinus of Valsalva of the LV, achieving a localization accuracy of 11.9 mm (Fig. 6C) and 9.3 mm (Fig. 6D), respectively.

Discussion

The study has demonstrated that: 1) it was feasible to localize IVA origin sites on intracardiac EAMs of both ventricular chambers and neighboring vessels using the AAOL system; 2) the AAOL system achieved a mean localization accuracy of 3.6 mm; 3) the AAOL system accurately predicted IVA origin sites in the RV, aortic root and papillary muscles; and 4) a predicted IVA origin site can be displayed on a patient-specific intracardiac EAM geometry for a potential ablation target guidance. We tested the localization accuracy of the new AAOL system on two commercial mapping systems (Carto 3 and EnSite ™ Precision mapping systems). Finally, we demonstrated the utility of the system in a cohort of patients from two different clinical centers. Should the AAOL system be integrated into an EAM system, it would achieve data collection and localization analysis in real time, and the expectation is that accurate localization of the IVA origin site using the proposed system would significantly shorten the procedure time.

In the study, we used 2 sets of pacing sites. Distribution #1 was a set of pacing sites at the discretion of the operator, as they would be placed during the procedure. Distribution #2 consisted of 10 pacing sites from Distribution #1 that were closest to IVA origin. We compared the AAOL prediction for these 2 pacing sites distributions, and there was no statistical difference between the predicted IVA locations. This demonstrated that the AAOL system does not require a good estimate of the neighbourhood of the site of origin, as it thus less dependent on operator choices. At present, the PaSo™ module (Biosense Webster, Inc., Irvine, CA) and the AutoMap module (EnSite ™ Precision, Abbott, St. Paul, MN) provide quantitative matching of ECG morphologies (19–20). Although the PaSo™ module or the AutoMap module is efficiently used in a clinical electrophysiology study, they do not derive localization information (20). Our AAOL system utilizes the same pacing data used by PaSo™ or AutoMap during the ablation procedure to localize the site of origin of IVAs, highlighting the clinical utility of the AAOL system.

The localization error range obtained here is narrow (3.6 mm) for diverse PVC/VT locations, illustrating the capability of this system. To the best of our knowledge, no other ECG method is available to locate IVA origin sites within 3.6 mm localization accuracy. The advantage of this system is its ability to achieve precise localization on the clinical intracardiac patient-specific EAM using 3-lead ECGs (III, V2 and V6) and several known pacing sites. We have previously shown that, using the intraprocedural SOLO system based on standard 12-lead ECG recordings, spatial localization of the site of early LV activation can be achieved without significant loss of accuracy in comparison to a 120-lead ECG imaging (ECGI) technique (21). Studies using a commercially available ECGI system recorded body surface potentials from 252 electrodes to identify noninvasively the site of focal activation and showed a median localization error of 20.7 mm in 9 pigs (22). Duchateau et al compared ECGI with invasive epicardial mapping, and found a poor correlation between the two modalities, with an average distance of 75 mm from the invasively mapped focal breakthrough locations to the predicted origin sites (23). Compared to the ECGI system, the AAOL system takes advantage of invasive mapping from known intracardiac sites to generate predicted locations of ventricular arrhythmias. It does not require pre-procedure imaging, and does not rely on the assumptions required for inverse

solution calculation (e.g. volume conductor, source model representation). For patients with multiple clinical IVAs, the collected sites of pace mapping can be repeatedly utilized to predict different IVA origin sites, which would decrease pace-mapping expense as shown in patient #7. If the IVAs are in the same neighbourhood, it might be possible to predict the location of more than one IVA when using the same pacing sites.

Although activation sequence mapping is more accurate (7) as compared to pace mapping, it requires relatively frequent spontaneous clinical ectopy. The pace-mapping method is the only available method to identify the site of IVA origin when activation mapping cannot be performed due to low PVC burden. However, pace-mapping is less helpful in identifying papillary muscle IVA origin sites because a papillary muscle IVA origin site may be far away from a site with the best pace map (25). Furthermore, previous studies have demonstrated that the pace mapping method may be inaccurate when the excellent pacing-match site is more than 2 cm away from the site of PVC origin (25). In this study, in several cases the pacing site with the highest correlation score was more than 1.5 cm away from the AAOL-predicted site and the site of successful ablation. Therefore, the new AAOL system offers an important improvement for the pace-mapping method to localize the IVT/PVC origins.

In this study, we developed a new intraprocedural automated system for localizing IVA origin sites. It built on a previous system, the SOLO system. The original SOLO system relied on acquisition of a complete EAM geometry with a smooth surface to achieve high localization accuracy, which made it difficult to use for RV site localization because of irregularities in RV EAM geometry. The new AAOL system uses the EAM geometry triangular mesh, with the mesh node nearest the tip of the predicted location defining the projected location. This critical modification from the original SOLO system overcomes limitations that led to inaccuracies when seeking to identify the site of origin of IVAs in the RV, aortic root, and internal ventricular structures such as the papillary muscles. As demonstrated in the present study, the AAOL system can determine IVA sites in these more challenging regions with similar accuracy as for typical LV endocardial sites.

Limitations

There are several limitations of this study. First, the study size is small, however we were able to demonstrate the accuracy of the new method in IVA arising at a number of cardiac structures. While these findings are promising, larger studies in expanded patient populations will increase the confidence in the method. A multicenter study is currently ongoing to assess the technique in guiding VA ablation. Second, the AAOL system assumes pacing is performed in the same chamber, including epicardial and vascular structures, as the arrhythmia. For patient #10 where the PVC was arising from the distal CS, if the operating electrophysiologists only performed mapping endocardially, the AAOL system could predict a site that is located outside the complete endocardial geometry, which then signifies the PVC origin site is on the epicardium. As specified in the Methods, our AAOL system has the capability to distinguish RV and LV or endocardium and epicardium for predicting IVA origin sites. However, in our cohort, we did not have enough cases of LV summit or mid septal PVCs to demonstrate this capability. In addition, for the IVAs originating from

papillary muscles, the localization accuracy was limited due to the complex structure and shape of the papillary muscles. Further studies are needed to assess whether our AAOL system could accurately localize the site of origin of papillary muscle IVAs onto 3D papillary muscle geometries reconstructed using the CartoSound™ module (Biosense Webster, Inc., Irvine, CA).

Conclusions

The AAOL system offers highly accurate localization of the site of PVC/IVT origin in both ventricular chambers and neighbouring vessels, which could potentially facilitate ablation procedures for patients with idiopathic ventricular arrhythmias.

Supplementary Material

Refer to Web version on PubMed Central for supplementary material.

Sources of Funding:

This work was supported by funding support from the Cardiac Arrhythmia Network of Canada (CANet) Post-doc Fellowship to SZ, Heart Rhythm Society Post-doc Fellowship to SZ; Department of Medicine of Dalhousie University to AA, Maritime Heart Centre grant to AA; NIH [R01HL142496 and R01HL126802] to NT, Leducq 16CVD02 to NT; Robert E. Meyerhoff Professorship to JC

Abbreviations:

IVAs	idiopathic ventricular arrhythmias
IVTs	idiopathic ventricular tachycardias
PVCs	premature ventricular complexes
EAM	electroanatomic mapping
ECGI	ECG imaging
AAOL	automatic arrhythmia origin localization
RF	radiofrequency

References

1. Park KM, Kim YH, Marchlinski FE. Using the surface electrocardiogram to localize the origin of idiopathic ventricular tachycardia. Pacing Clin Electrophysiol 2012;35:1516–27. [PubMed: 22897344]
2. Gaztanaga L, Marchlinski FE, Betensky BP. Mechanisms of cardiac arrhythmias. Rev Esp Cardiol (Engl Ed) 2012;65:174–85. [PubMed: 22192903]
3. Pathak RK, Ariyarathna N, Garcia FC, et al. Catheter Ablation of Idiopathic Ventricular Arrhythmias. Heart Lung Circ 2019;28:102–209. [PubMed: 30554597]
4. Cronin EM, Bogun EM, Maury P, et al. 2019 HRS/EHRA/APHRS/LHRS expert consensus statement on catheter ablation of ventricular arrhythmias. Heart Rhythm 2019;17:e2–e154. [PubMed: 31085023]

5. Dukkipati SR, Choudry S, Koruth JS, et al. Catheter Ablation of Ventricular Tachycardia in Structurally Normal Hearts: Indications, Strategies, and Outcomes-Part I. J Am Coll Cardiol 2017;70:2909–2923. [PubMed: 29216987]
6. Ito S, Tada H, Naito S, et al. Development and validation of an ECG algorithm for identifying the optimal ablation site for idiopathic ventricular outflow tract tachycardia. J Cardiovasc Electrophysiol 2003;14:1280–6. [PubMed: 14678101]
7. Betensky BP, Park RE, Marchlinski FE, et al. The V(2) transition ratio: a new ectrocardiographic criterion for distinguishing left from right ventricular outflow tract tachycardia origin. J Am Coll Cardiol 2011;57:2255–62. [PubMed: 21616286]
8. Efimova E, Dinov B, Acou WJ, et al. Differentiating the origin of outflow tract ventricular arrhythmia using a simple, novel approach. Heart Rhythm 2015;12:1534–40. [PubMed: 25847476]
9. Asatryan B, Ebrahimi R, Strebel I, et al. Man vs Machine: Performance of Manual vs Automated ECG Analysis for Predicting the Chamber of Origin of Idiopathic Ventricular Arrhythmia. J Cardiovasc Electrophysiol 2019;31:410–416. [PubMed: 31840899]
10. Jamil-Copley S, Bokan R, Kojodjojo P, et al. Noninvasive electrocardiographic mapping to guide ablation of outflow tract ventricular arrhythmias. Heart Rhythm 2014;11:587–594. [PubMed: 24440381]
11. Wissner E, Revishvili A, Metzner A, et al. Noninvasive epicardial and endocardial mapping of premature ventricular contractions. Europace 2017;19; 843–849. [PubMed: 27207812]
12. Erkapic D, Neumann T. Ablation of Premature Ventricular Complexes Exclusively Guided by Three-Dimensional Noninvasive Mapping. Card Electrophysiol Clin 2015;7:109–115. [PubMed: 25784027]
13. Graham AJ, Orini M, Zacur E, et al. Evaluation of ECG Imaging to Map Haemodynamically Stable and Unstable Ventricular Arrhythmias. Circ Arrhythm Electrophysiol 2020 1 14 [Epub ahead of print].
14. Sapp JL, Bar-Tal M, Howes AJ, et al. Real-time localization of ventricular tachycardia origin from the 12-lead electrocardiogram. JACC Clin Electrophysiol 2017;3:687–699. [PubMed: 29759537]
15. Zhou S, AbdelWahab A, Horack BM, et al. Prospective Assessment of An Automated Intraprocedural 12-lead ECG-Based System for Localization of Early Left Ventricular Activation. Accepted to Circ Arrhythm Electrophysiol on March 31st, 2020.
16. Yamada T, Kay GN. Anatomical consideration in catheter ablation of idiopathic ventricular arrhythmias. Arrhythmia Electrophysiol Rev 2016;5:203–9.
17. Kemmelings JG, Linnenbank AC, Muilwijk SL, et al. Automatic QRS onset and offset detection for body surface QRS integral mapping of ventricular tachycardia. IEEE Trans Biomed Eng 1994;41:830–836. [PubMed: 7959810]
18. Shirai Y, Liang JJ, Santangeli P, et al. Catheter ablation of premature ventricular complexes with low intraprocedural burden guided exclusively by pace-mapping. J Cardiovasc Electrophysiol 2019;30:2326–2333. [PubMed: 31424129]
19. Széplaki G, Tahin T, Szilágyi SZ, et al. Ablation of premature ventricular complexes originating from the left ventricular outflow tract using a novel automated pace-mapping software. Interv Med Appl Sci. 2010;2:181–3.
20. Zhou S, Sapp JL, Horacek BM, et al. Automated Intraprocedural Localization of Origin of Ventricular Activation Using Patient-Specific Computerized Tomography Imaging. Heart Rhythm. 2019;17:567–575. [PubMed: 31669770]
21. Zhou S, Sapp JL, AbdelWahab A, et al. of ventricular activation origin using patient-specific geometry: Preliminary results. J Cardiovasc Electrophysiol 2018;29:979–986. [PubMed: 29702740]
22. Hohmann S, Rettmann ME, Konishi H, et al. Spatial Accuracy of a Clinically Established Noninvasive Electrocardiographic Imaging System for the Detection of Focal Activation in an Intact Porcine Model. Circ Arrhythm Electrophysiol 2019 11 11 [Epub ahead of print].
23. Duchateau J, Sacher F, Pambrun T, et al. Performance and limitations of noninvasive cardiac activation mapping. Heart Rhythm 2019;16:435–442. [PubMed: 30385382]

24. Zhou S, Sapp JL, Horacek BM, et al. Automated Intraprocedural Localization of Origin of Ventricular Activation Using Patient-Specific Computerized Tomography Imaging. Heart Rhythm 2019;17:567–575. [PubMed: 31669770]

25. Bogun F, Taj M, Ting M, et al. Spatial resolution of pace-mapping of idiopathic ventriculart achycardia/ectopy originating in the right ventricular outflow tract. Heart Rhythm 2008;5:339–44. [PubMed: 18313589]

Perspectives

Competency in Medical Knowledge

Catheter ablation of the Idiopathic ventricular arrhythmias (IVAs) can be enhanced by accurately identifying the site of origin of the IVA. The new automatic arrhythmia origin localization (AAOL) system is capable of localizing the site of origin of earliest activation in either ventricle using 3-lead ECGs, potentially facilitating catheter ablation procedures for patients with IVAs.

Translational Outlook

In this pilot study, the AAOL system localized the site of origin of earliest activation in patients with IVAs. The AAOL algorithm will need to be integrated into an existing electroanatomic mapping system to fully assess its clinical utility. Prospective, randomized studies are needed to ascertain the clinical value of the AAOL system.

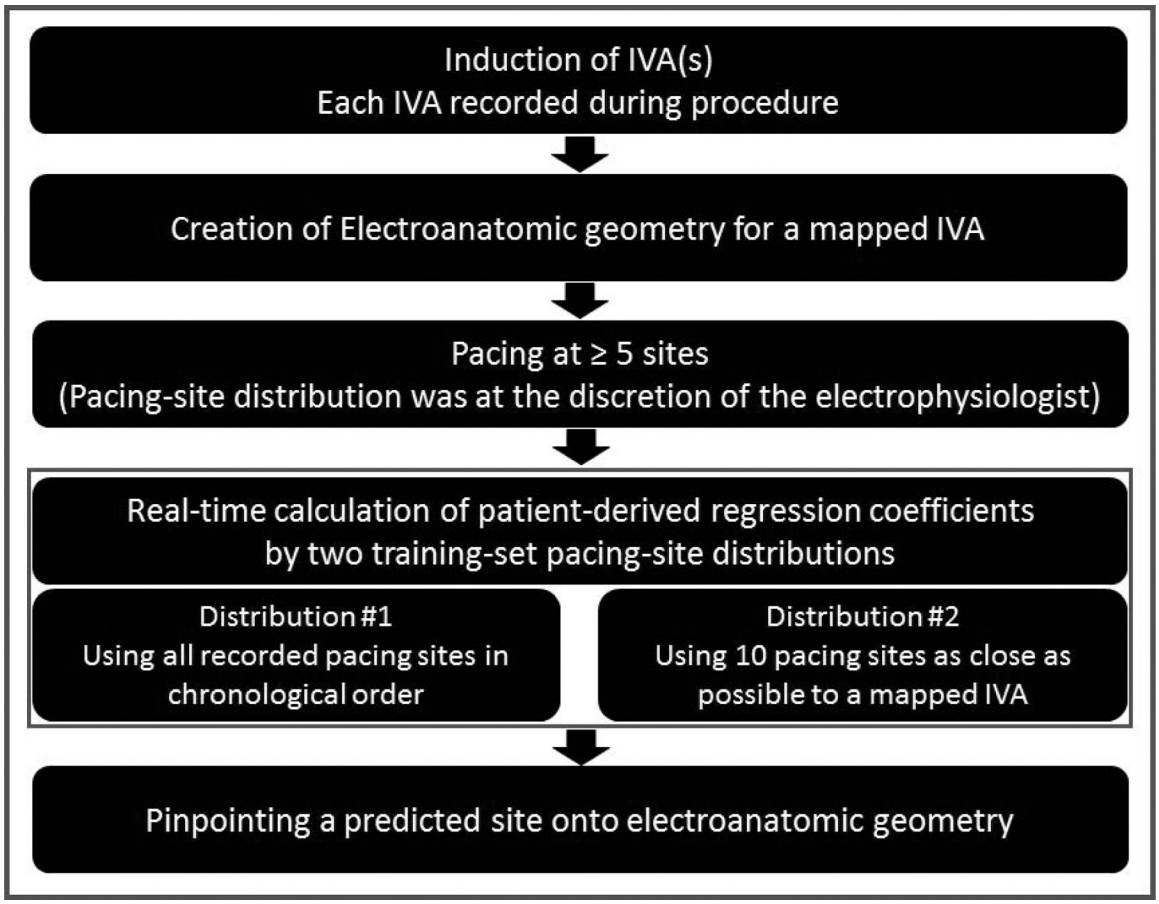

Figure 1.
A clinical workflow to integrate the AAOL system during IVA procedure of catheter ablation. IVA indicates idiopathic ventricular arrhythmias.

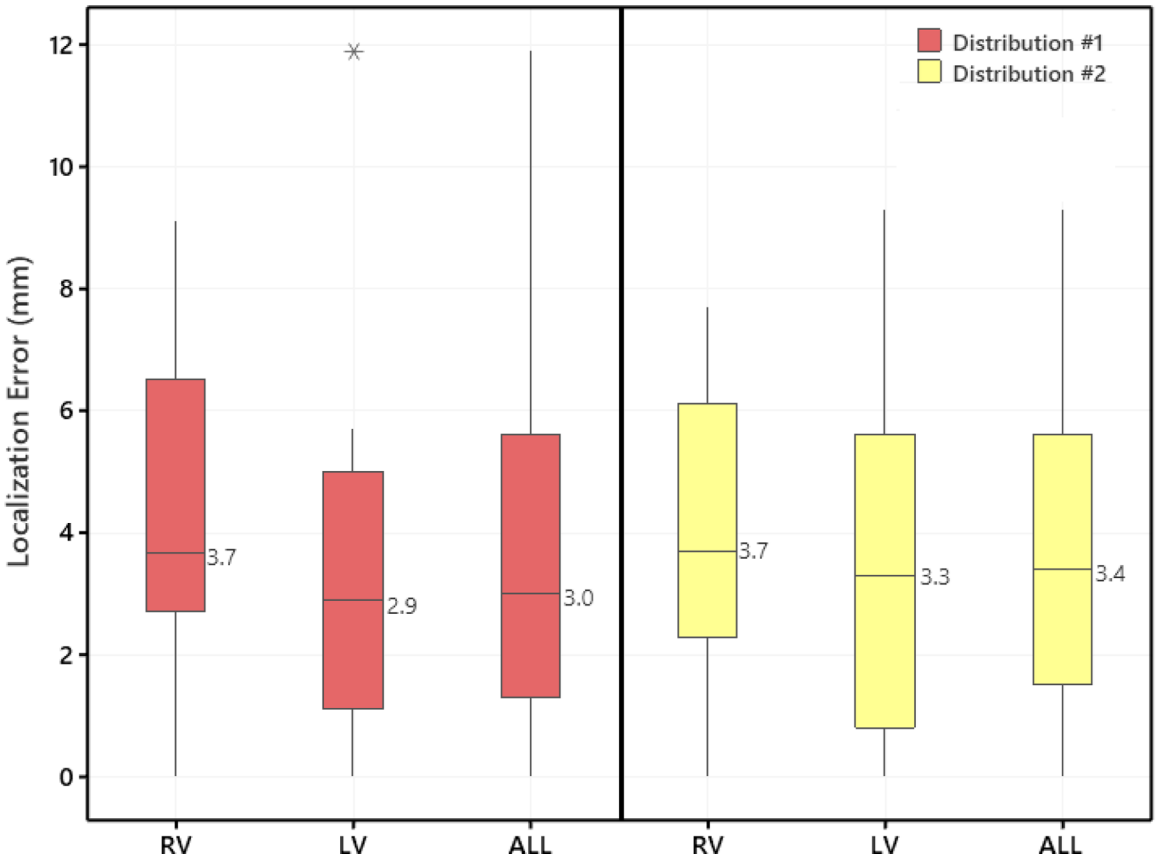

Figure 2.

Localization errors between clinically-identified IVA origin site and the site predicted by the AAOL system using two pacing-site distributions, per cardiac chamber. Distribution #1 was to use all recorded pacing sites of a mapped IVA (in chronological order) to compute the identified PVC/VT origin site; Distribution #2 was to use 10 neighboring pacing sites of an identified IVA origin site to compute the identified PVC/VT origin site. Boxes represent interquartile range, error-bars represent range, and line in the box indicates median. The ALL plot represents the aggregate of all IVAs across all chambers. RV indicates right ventricle; and LV, left ventricle.

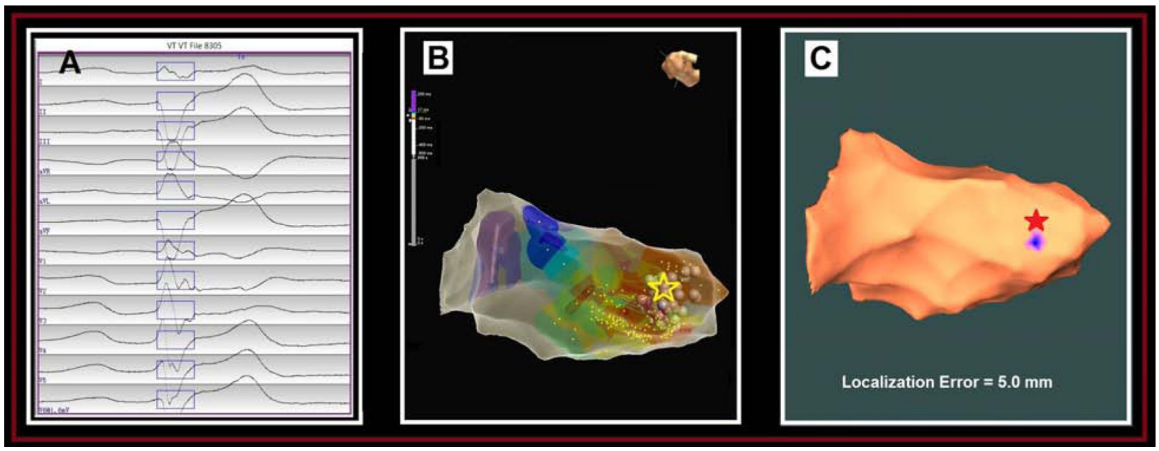

Figure 3.

Localization of a papillary muscle PVC origin site by the AAOL system: (A) shows the recorded 12-lead ECG of PVC during the procedure for patient #6. The onset of one PVC beat was automatically detected (17); the user can edit the onset of the 120-ms window (rectangle box) if correction is necessary. (B) illustrates the endocardial local-activation-time (LAT) EAM for this patient, with the site of PVC origin site (identified by activation mapping) depicted by the yellow star. (C) shows that using the AAOL system to predict the PVC origin site indicated by the blue patch onto the EAM geometry, with the actual site of PVC origin marked by the red star. Localization error of PVC origin site is 5.0 mm.

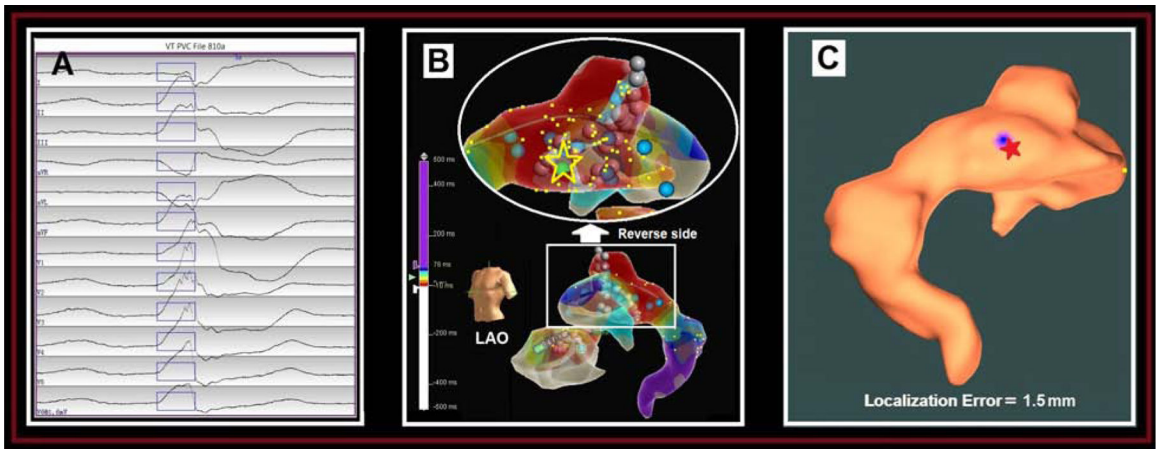

Figure 4.

Localization of a distal coronary sinus (CS) PVC origin site by the AAOL system: (A) shows the recorded 12-lead ECG of PVC during the procedure for patient #10. The onset of one PVC beat was automatically detected (17); the user can edit the onset of the 120-ms window (rectangle box) if correction is necessary. (B) illustrates the patient-specific CS EAM, with the site of PVC origin site (identified by activation mapping) depicted by the yellow star and green ball. (C) shows that using the AAOL system to predict a PVC origin site indicated by the blue patch onto the EAM geometry, with the actual site of PVC origin marked by the red star. Localization error of PVC origin site is 1.5 mm. Yellow dots indicate recorded pacing sites on the EAM geometry.

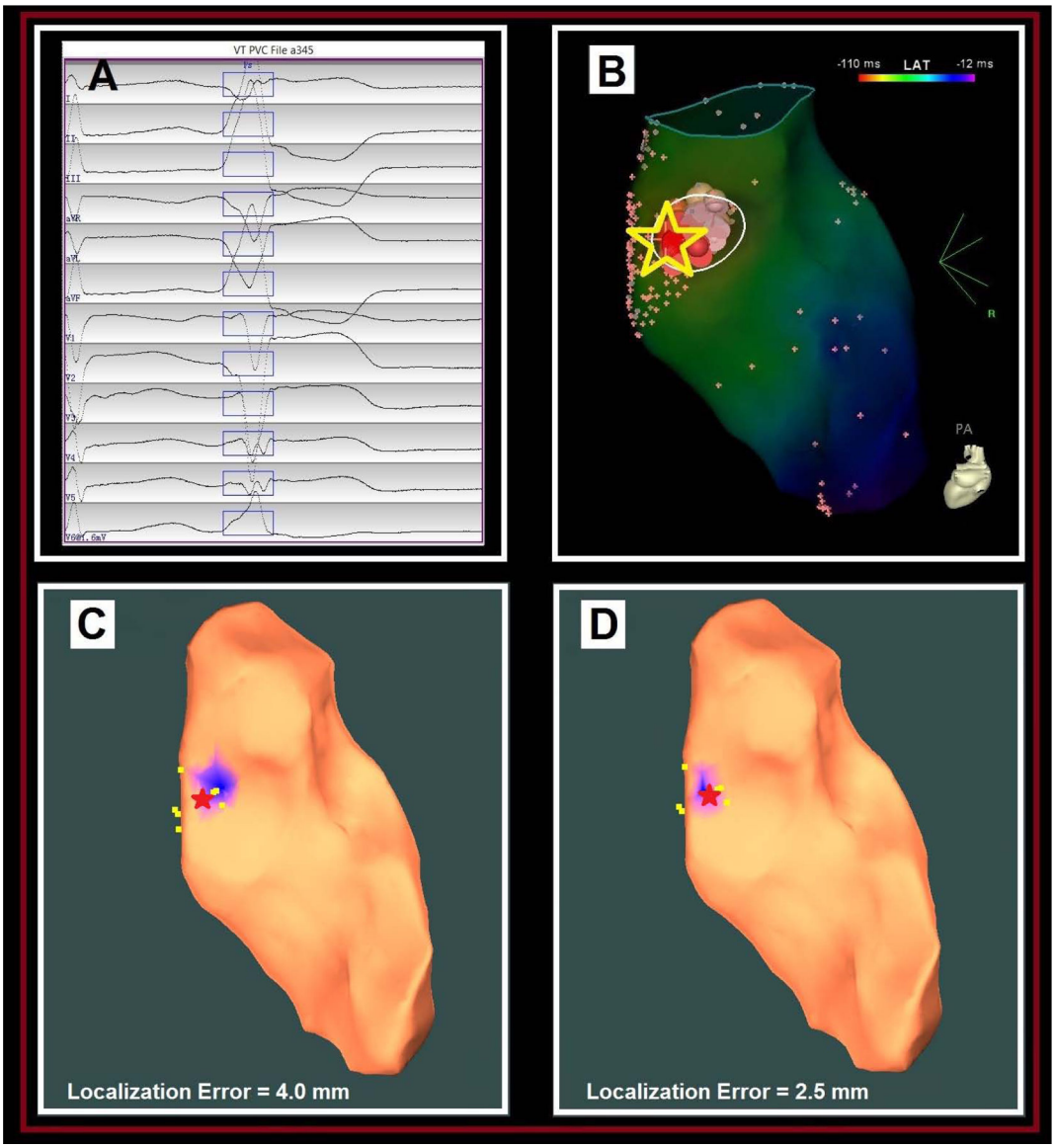

Figure 5.

Localization of a septal RVOT PVC origin site by the AAOL system: (A) shows the recorded 12-lead ECG of a PVC during the procedure for patient #12. The onset of one PVC beat was automatically detected (17); the user can edit the onset of the 120-ms window (rectangle box) if correction is necessary. (B) illustrates the endocardial EAM local-activation-time (LAT) map of RVOT for this patient, with the site of PVC origin (identified by activation mapping) depicted by the yellow star. (C) shows that the AAOL system was used to predict a PVC origin site marked in the blue patch onto the RVOT EAM geometry when using all recorded pacing sites of the PVC (Distribution #1), having a localization error of 4.0 mm in comparison with the actual PVC origin site indicated by the red star. Yellow dots indicate recorded pacing sites on the EAM. (D) shows that the AAOL system was used to predict a PVC origin site marked in the blue patch onto the RVOT EAM geometry after including up to 10 nearest pacing sites of the actual PVC origin site marked

by the red star (Distribution #2), achieving a localization accuracy of 2.5 mm. Yellow dots indicate recorded pacing sites on the EAM.

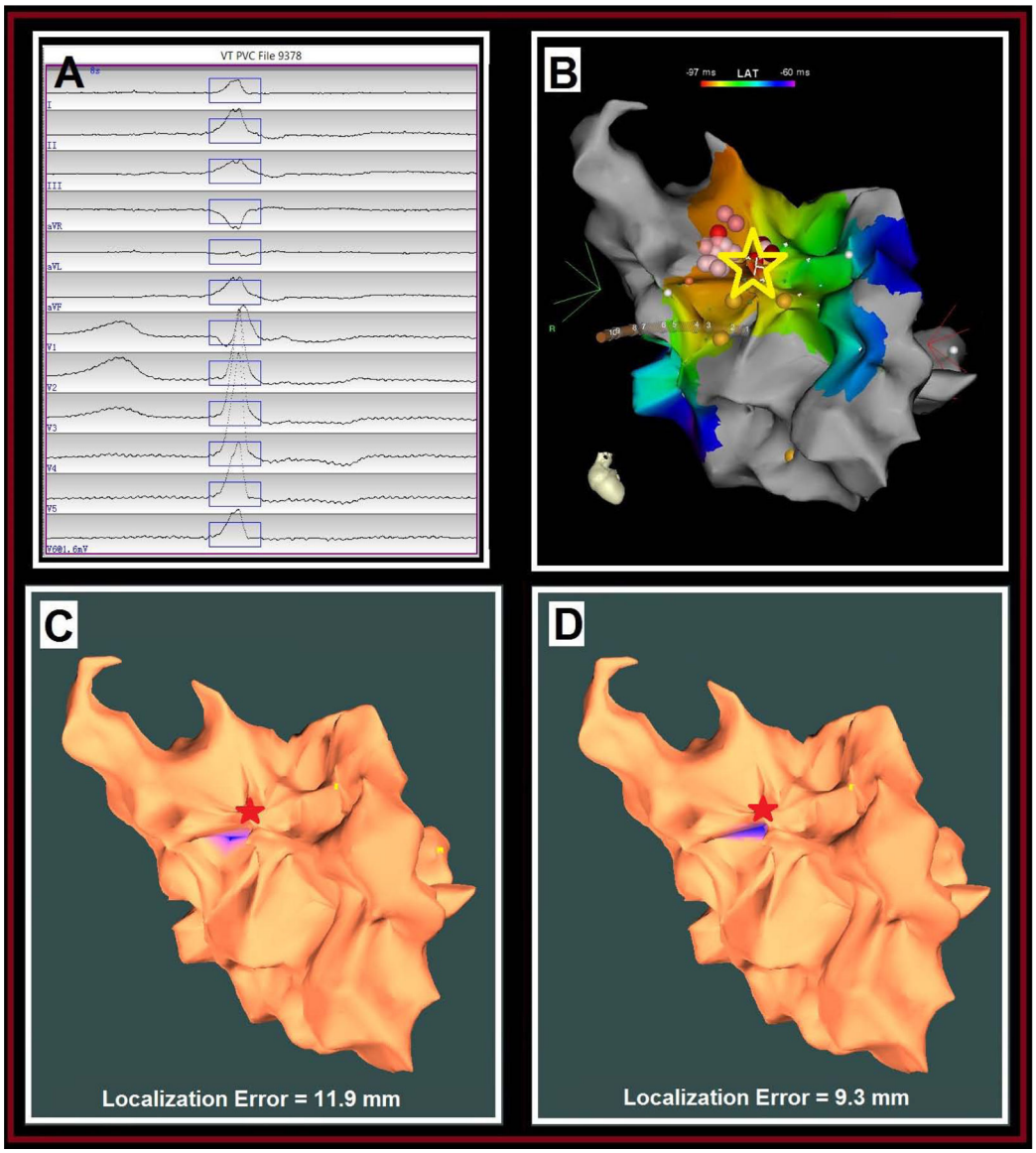

Figure 6.

Localization of an aortic PVC origin site by the AAOL system: (A) shows the recorded 12-lead ECG of mapped PVC morphology during the procedure for patient #17. The onset of one PVC beat was automatically detected (17); the user can edit the onset of the 120-ms window (rectangle box) if correction is necessary. (B) illustrates the endocardial EAM LAT map of right sinus of Valsalva for this patient, the site of PVC origin (identified by activation mapping) depicted by the yellow star. (C) shows that the AAOL system was used to predict a PVC origin site marked in the blue patch onto the EAM geometry of right sinus of Valsalva when using all recorded pacing sites of the PVC (Distribution #1), having a localization error of 11.9 mm in comparison with the actual PVC origin site indicated by the red star. Yellow dots indicate recorded pacing sites on the EAM. (D) shows that the AAOL system was used to predict a PVC origin site marked in the blue patch onto the EAM geometry of right sinus of Valsalva after including up to 10 nearest pacing sites of the actual PVC origin

site marked by the red star (Distribution #2), achieving a localization accuracy of 9.3 mm. Yellow dots indicate recorded pacing sites on the EAM.

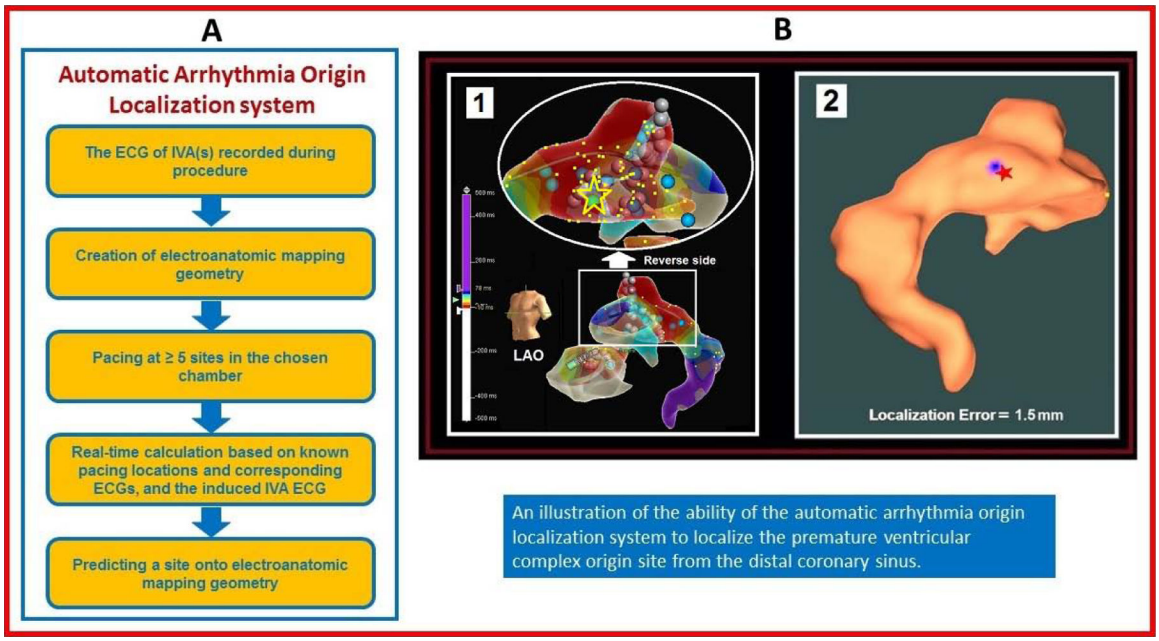

Central Illustration. A New Intraprocedural Automatic Arrhythmia Origin Localization (AAOL) System for Localizing IVA Origin Sites

(A) Automatic Arrhythmia Origin Localization (AAOL) was designed to localize the site of origin of idiopathic ventricular arrhythmias (IVAs) during catheter ablation. (B) Localization of a distal coronary sinus (CS) premature ventricular complex (PVC) origin site by the AAOL system: (1) illustrates the patient-specific CS electroanatomic mapping (EAM) with left anterior descending (LAO) view, with the PVC origin site (identified by activation mapping) depicted by the yellow star and green ball. (2) shows that using the AAOL system to predict a PVC origin site indicated by the blue patch on the EAM geometry, with the actual PVC origin site marked by the red star. Yellow dots indicate recorded pacing sites on the EAM geometry.

Table 1.

Clinical characteristics of 20 IVA patients

Clinical Characteristics	Number (%)
Male	14 (70.0)
Age (years)	59.5 ± 19.6 years
Type of arrhythmia	
PVC	9 (45.0)
VT	4 (20.0)
PVC/VT	7 (35.0)
ICM	4 (20.0)
Heart failure	3 (15.8)
ICD present	2 (10.5-)
CRTD present	1 (5.3)

IVA = idiopathic ventricular arrhythmia; Age (years) represented as Mean ± Standard Deviation; PVC = premature ventricular contraction; VT =ventricular tachycardia; ICM = Ischemic cardiomyopathy; ICD = implantable cardioverter-defibrillator; CRTD = cardiac resynchronization therapy defibrillator

Table 2.

Clinical Mapped IVA origin sites

Patient #	Mapped PVC/VT	Clinically Identified Origin Site	Ablation Localization	AM	PM	SA	Ablation Successful?
1	PVC	Posteroseptal RVOT	Posteroseptal RVOT and the left and right coronary cusp commissure	✓			Partial
2	PVC	Basal anterolateral wall of the left ventricle, adjacent to the mitral valve	Basal anterolateral wall of the left ventricle, adjacent to the mitral valve	✓			Partial
3	PVC	Posteromedial papillary muscle	Posteromedial papillary muscle	✓			YES
4	PVC	Posteromedial papillary muscle	Posteromedial papillary muscle		✓		YES
5	VT	RV moderator band	N/A		✓		NA
6	PVC	Posteromedial papillary muscle	Posteromedial papillary muscle	✓			YES
7	PVC1	RV moderator band	RV moderator band	✓			YES
	PVC2	Septal side of the moderator band and apical septal insertion side	Septal side of the moderator band and apical septal insertion side	✓			YES
8	PVC1	Posteromedial papillary muscle	Posteromedial papillary muscle	✓			YES
	PVC2	Slightly more lateral to posteromedial papillary muscle	Posteromedial papillary muscle	✓			YES
	PVC3	Right coronary cusp in LVOT	Right coronary cusp in LVOT	✓			YES
9	PVC	Posteromedial papillary muscle	Posteromedial papillary muscle	✓			YES
10	PVC	Distal CS	Within the distal CS and LV endocardium directly opposite the earliest site in the CS	✓			YES
11	PVC	AMC	AMC	✓			YES
12	PVC	Septal RVOT	Septal RVOT	✓			YES
13	PVC	Lateral RVOT	Lateral RVOT	✓			YES
14	VT	AMC	AMC		✓		YES
15	PVC	RVOT free wall	RVOT free wall	✓			YES
16	PVC	Septal tricuspid valve papillary muscle	Right ventricular septum	✓			YES
17	PVC	Right coronary cusp in LVOT	Right coronary cusp in LVOT	✓			YES
18	PVC	Posteromedial papillary muscle	Posteromedial papillary muscle	✓			YES
19	PVC	LV crux	LV crux	✓			YES
20	PVC	Anterior surface of the posteromedial papillary muscle	Anterior surface of the posteromedial papillary muscle			✓	YES

IVA = idiopathic ventricular arrhythmia; PVC = premature ventricular complex; IVT = idiopathic ventricular tachycardia; EAM = electroanatomic mapping; AM = activation mapping; PM = pace-mapping; SA = suppression with ablation; RVOT = right ventricular outflow tract; LVOT = left ventricular outflow tract , RV = right ventricular; CS = coronary sinus; AMC = aorto-mitral continuity; LV= left ventricular. The PVC/IVT origin site was clinically identified by AM/PM/SB is given by ✓. NA defined no ablation performed in this case due to given clinical significance of PVC was not known, and patient inability to tolerate the procedure.

Table 3.

Localization accuracy of the AAOL system

Patient #	Mapped PVC/VT	# of pacing sites	Anatomic geometry	10 nearest Pacing Sites	Distribution #1 Localization Error (mm)	Distribution #2 Localization Error (mm)	Highest Correlation Score (%)	Highest Correlation Site to AAOL Site (mm)
1	PVC	14	EAM	10	9.1	7.7	—	—
2	PVC	10	EAM	10	3.3	3.3	90.1	10.1
3	PVC	17	EAM*	10	2.7	4.6	95.9	3.6
4	PVC	16	EAM	10	0.0	0.0	92	8.5
5	VT	18	EAM	10	2.7	2.2	98.0	2.7
6	PVC	8	EAM	8†	5.0	5.0	—	—
7	PVC1	9	EAM	9†	0.0	0.0	—	—
	PVC2	(9+3)**	EAM	10	6.6	6.6	—	—
8	PVC1	20	EAM*	10	0.0	0.0	—	—
	PVC2	11	EAM*	10	1.1	0.0	—	—
	PVC3	19	EAM	10	3.9	3.9	94.5	4.0
9	PVC	16	EAM	10	2.9	3.0	94.3	2.9
10	PVC	9	EAM	9†	1.5	1.5	95	17.6
11	PVC	7	EAM	7†	5.6	5.6	—	—
12	PVC	14	EAM	10	4.0	2.5	97.2	12.7
13	PVC	11	EAM	10	6.2	4.6	—	—
14	VT	16	EAM	10	3.0	2.6	92.4	3.0
15	PVC	14	EAM	10	2.7	4.0	97.1	14.3
16	PVC	19	EAM	10	3.3	3.4	86.2	16.6
17	PVC	12	EAM	10	11.9	9.3	94.7	7.5
18	PVC	22	EAM*	10	1.3	5.9	87.7	16.4
19	PVC	8	EAM	8†	5.7	5.7	—	—
20	PVC	10	EAM	10	0.8	0.8	97.4	20.5

IVA = idiopathic ventricular arrhythmia; PVC = premature ventricular complex; VT = ventricular tachycardia; AAOL = Automatic Arrhythmia Origin Localization. Distribution #1 used use all recorded pacing sites to localize the site of a mapped PVC/VT origin. Distribution #2 used the 10 nearest pacing sites of an identified PVC/VT origin site to compute the identified PVC/VT origin site. Highest Correlation Score defined the highest percent correlation between the PVC/IVT morphology and pacing-site ECG morphologies using the PaSo™ module (Carto 3 system, Biosense webster, Diamond Bar, CA) or the AutoMap module (EnSite™ Precision, Abbott, St. Paul, MN). The distance from the site with the highest correlation score to the AAOL-predicted site (based on Distribution #1) was calculated. '—' defined no PaSo module or AutoMap module performed. EAM = electroanatomic;

'*' integrated geometry of intracardiac echocardiography imaging and the EA map.

'†' fewer than 10 pacing sites were available.

'**' defines a set of pacing sites that consists of previous 9 pacing sites from mapping PVC1 and the recorded 3 additional pacing sites from mapping PVC2.